LBL-24177
UC-94c

Lawrence Berkeley Laboratory
UNIVERSITY OF CALIFORNIA

APPLIED SCIENCE DIVISION

RECEIVED
LAWRENCE
BERKELEY LABORATORY

FEB 1 1988

LIBRARY AND
DOCUMENTS SECTION

Corrosion, Passivity, and Breakdown of Alloys Used in High Energy Density Batteries: Final Report

J. Kruger

October 1987

TWO-WEEK LOAN COPY
This is a Library Circulating Copy
which may be borrowed for two weeks.

APPLIED SCIENCE
DIVISION

LBL-24177 c.2

Prepared for the U.S. Department of Energy under Contract DE-AC03-76SF00098

DISCLAIMER

This document was prepared as an account of work sponsored by the United States Government. While this document is believed to contain correct information, neither the United States Government nor any agency thereof, nor the Regents of the University of California, nor any of their employees, makes any warranty, express or implied, or assumes any legal responsibility for the accuracy, completeness, or usefulness of any information, apparatus, product, or process disclosed, or represents that its use would not infringe privately owned rights. Reference herein to any specific commercial product, process, or service by its trade name, trademark, manufacturer, or otherwise, does not necessarily constitute or imply its endorsement, recommendation, or favoring by the United States Government or any agency thereof, or the Regents of the University of California. The views and opinions of authors expressed herein do not necessarily state or reflect those of the United States Government or any agency thereof or the Regents of the University of California.

LBL-24177

CORROSION, PASSIVITY AND BREAKDOWN OF ALLOYS USED IN HIGH ENERGY DENSITY BATTERIES

Final Report

October 1987

by

Jerome Kruger

Department of Materials Science and Engineering
The Johns Hopkins University
Maryland Hall
Baltimore, Maryland 21218

for

Technology Base Research Project
Lawrence Berkeley Laboratory
University of California
Berkeley, California 94720

This work was supported by the Assistant Secretary for Conservation and Renewable Energy, Office of Energy Storage and Distribution of the U.S. Department of Energy under Contract No. DE-AC03-76SF00098, Subcontract No. 4539610 with the Lawrence Berkeley Laboratory.

I. Introduction

The objective of this research is to further the understanding of the passivity of metals and alloys in non-aqueous and mixed solvents. There is a lack of data in this area, despite its importance to applications such as the construction materials for high energy density batteries. There have been a number of corrosion-related problems reported in the construction materials of such batteries . As demands for longevity for these batteries increase, problems associated with corrosion will become increasingly important.

This work is concerned with analyzing the nature, mode of formation, and mode of breakdown of passive films that exist on alloys in non-aqueous and mixed solvents. Work during Year I has concentrated upon generating cyclic voltammograms and potentiodynamic curves as baseline data on Au and Armco Fe in water/propylene carbonate mixtures. In addition, Scanning Electron Microscopy has been performed in order to characterize the attack observed and to correlate it to the electrochemical parameters measured.

II. Results and Discussion

Some work performed during Year I has been concerned with electrolyte characterization via electrochemical studies on Au. Solutions containing 0, 10 and 50 mole % propylene carbonate (PC) with a supporting electrolyte of 0.5 M $LiClO_4$ have been studied. The first two solutions have been studied both by cyclic voltammetry and potential sweep techniques, while the 50 mole % solution has so far only been studied via the single potential sweep technique. All solutions were made from high purity water from a Millipore Milli-Q Water System which delivers water with a resistivity of 18 MΩ–cm, anhydrous $LiClO_4$ (99.95%) and anhydrous LiCl (99.985 %) from Johnson-Matthey, and 99% PC from Alfa Products. The gold electrode was 99.998% Au from Johnson-Matthey. All solutions were deaerated for at least two hours with dry nitrogen gas. The cyclic voltammograms were generated at a scan rate of 40 mV/sec while the single potential sweeps were performed at 0.1 mV/sec.

A summary of the cyclic voltammograms is shown in Figure 1. The potentiodynamic scans are overlaid in Figure 2. Potentiodynamic scans were also performed on Au in the above solutions after the

addition of 0.01 M LiCl. These comparisons are shown in Figures 3 - 5. Examination of these figures shows that changes take place in both the cyclics and in the single potential sweep curves upon the addition on PC. In the cyclics, a set of anodic waves can be seen beginning at about +0.3 V(SCE), with a corresponding cathodic wave appearing during the reverse scan. Additional reduction peaks are seen superimposed upon the hydrogen evolution reaction, at -0.3 V(SCE) and -0.5 V(SCE). While cyclic voltammograms have not been performed as yet on the 50 mole % PC solution, inspection of the single potential sweep curves in Figure 2 shows that it appears that the 10 mole % and 50 mole % solutions have very similar behavior, possibly due to a saturation of surface sites for PC at 10 mole %. Since PC should be stable at these potentials, it is suspected that the increased currents are due to either adsorption of PC or oxidation of an impurity in the commercial grade PC. Work at Tel Aviv University, under a sub-cotract from Hopkins, is pursuing this possibility.

The effect of 0.01 M Cl^- ion as LiCl has been investigated by potentiodynamic polarization. The results are displayed in Figures 3 - 5. Figure 3 shows the curves for Au in pure water and with the addition of 0.01 M Cl^-. Over most of the potential range studied, Au is film-free. In none of the cases studied does Cl^- ion have a marked effect below +0.51 V(SCE), the reversible potential for Au oxide formation. This is expected since the predominant role of Cl^- ions is to interfere with passive surface films. However, in the case of 50 mole % PC, there is a significant increase in the current. This may be due to interference by Cl^- in the formation of the Au oxide. The lack of such an effect at lower PC levels may point to a synergistic role for PC in oxide film formation in these solutions.

Future work on gold will focus on using cyclic voltammetry to understand the origins of the changes observed upon the addition of PC and LiCl without complications due to faradaic reactions of the electrode. Different scan rates will be used in order to determine what type of diffusion process is controlling the adsorption of PC. Impedance measurements will also be made in order to understand the adsorption process.

Armco iron (99.9% Fe) was obtained from Metal Samples, Inc., in the form of 5/8" diameter, 1/8" thick disks. These disks were first wet polished through 800 grit silicon carbide paper. The samples were then ultrasonically degreased in methanol and then high purity water before immersion in the 0.5 M

$LiClO_4$ solution. The solution was then deaerated with dry nitrogen for at least two hours. At that point, the corrosion potential was measured and a potentiodynamic scan was begun at -.1 V electronegative to E_{corr} , scanning anodically at a rate of 1 mV/sec.

Experimental work has focussed upon interpretation of the electrochemical data generated for Armco Fe and 1018 steel in solutions of varying amounts of PC and water with 0.5 M $LiClO_4$ as the electrolyte. In order to visualize the trends in the data as a function of solvent ratio, characteristic parameters were determined from each polarization curve and impedance spectrum. These data are presented in this report. A schematic polarization curve and a schematic impedance spectrum are shown in Figure 6 with the characteristic parameters of each indicated.

The polarization curve has five characteristic parameters : the corrosion potential determined during the scan ($E_{corr/scan}$), the primary passivation potential (E_{pp}), the breakdown potential (E_b), the peak passivation current density (i_{pp}), and the passive current density (i_{pass}). In addition, the corrosion potential was measured in all solutions prior to the scan with a saturated calomel electrode (SCE). The potential at which the current changed polarity was designated $E_{corr/scan}$. In most cases it corresponded quite closely (typically within 40 mV) with the E_{corr} measured at open circuit before the start of the scan. Cases where it did not will be discussed below. E_{pp} was defined as the potential at the nose of the passivation curve, and in conjunction with i_{pp} relates to the ease with which a passive film can be formed on a material in a given solution. The magnitude of i_{pass} gives information concerning the protectiveness of the passive film. E_{bd} relates to the passive film's ability to resist breakdown. The more electropositive the value, the more resistant is the material to breakdown of the passive film.

The impedance spectrum of Figure 6b has three parameters of interest. The first is R_Ω which corresponds to the solution resistance between the tip of the Luggin capillary and the metal surface and is therefore related to the solution conductivity. The polarization resistance, R_p , can be related to the general corrosion rate of the metal under many conditions. Finally, the interfacial capacitance, C_{interf} , is due to the capacitance of the metal/solution interface and can give information on adsorption. While Figure 6b is for an ideal Randles' circuit, it should be emphasized that essentially all of the impedance spectra obtained so far in this study are well approximated by this model.

The dependence of the polarization curve parameters upon solution composition is shown in Figures 7 and 8. Data across the entire compositional range have been gathered for Armco Fe, and over most of the range for 1018 steel. Figure 7 shows the characteristic potentials as a function of mole % PC. For both materials, increasing PC content causes an electropositive shift in both E_{corr} and E_{pp} . For E_{pp} , there is only a slight shift on the aqueous-rich side, however, a shift of over 300 mV occurs upon moving from 50 mole % PC to 90 mole % PC. The shift in E_{corr} is smoother over the compositional range, though of roughly the same magnitude. For the case of E_b , there is little change on the aqueous-rich side of the binary mixture, though a slight increase is observed at 50 mole % PC. However, on the PC-rich side, a dramatic decrease in E_b is observed, indicating an increased susceptibility to localized attack.

Figure 8 illustrates the effect of solution composition on the two characteristic current density parameters, i_{pp} and i_{pass} . A smooth decrease in i_{pp} is observed upon an increase in PC level until a sudden decrease of almost 4 orders of magnitude occurs between 90 and 100 mole % PC. A smooth increase is found for i_{pass} on Armco Fe through 90 mole % PC, after which time a drop of 3 orders of magnitude is observed. It should be pointed out that in almost all cases the behavior of 1018 steel mimics that of Armco Fe for the characteristics measured in this study.

Recent work has also focussed upon the stability of the passive films formed in the various water/PC mixtures. It was found that for any solution with 30 mole % PC or more, a stable passive film was not formed upon the application of a potential step from E_{corr} to the middle of the passive range as determined by potentiodynamic testing. In fact, in all of those solutions ($\geq$ 30 mole % PC) severe pitting and general dissolution of the surface occurred during maintenance of the potential in the supposed passive range. Since the passivation of the surface in these solutions during potential scanning was reproducible, an investigation of the conditions necessary for passivation in 50 mole % PC was undertaken. Three potential control approaches were used.

(a) **Scan and Step** : Scan at 1 mV/sec to the nose of the passivation region (E_{pp}) and then step to the middle of the passive region (+0.75 V(SCE)). This tests the importance of active dissolution to the passivation process.

(b) **Step and Scan** : Step to E_{pp} , then scan at 1 mV/sec to +0.75 V(SCE). This tests the possibility of competing processes occurring on the metal surface bared during the active dissolution step.

(c) **Double Step** : Step to just above E_{pp} , wait for 10 minutes, and then step to +0.75 V(SCE). This tests the idea of the need for a precursor film before the "true" passive film can form.

Armco Fe in 50 mole % PC has an E_{pp} of -.116 V(SCE), i_{pp} of 18mA/cm^2 , i_{pass} of 45 μA/cm^2 , and an E_{bd} of +1.076 V(SCE). The Scan-and-Step test resulted in almost immediate pitting of the sample. Upon the step to +0.75 V, a decrease in the current to 1 mA/cm^2 occurred, but the current immediately began to rise and had reached 6 mA/cm^2 within 5 minutes, at which time the the test was terminated. The Step-and-Scan test was more successful with respect to the formation of a passive film. The scan following the step to Epp followed the characteristics of the scans begun at E_{corr} , indicating that the initial active dissolution was not a necessary condition for passivation. At +0.75 V, the current density was 30 μA/cm^2, which is actually slightly lower than the passive current density obtained after the scan from E_{corr} . However, within 1 hour, the current density had increased to 84 μA/cm^2, indicating a loss of some of the protective ability of the film. Post-test inspection of the surface showed that one region had indeed broken down and undergone widespread dissolution. The remainder of the surface showed some minor attack, probably due to time spent in the active region during the scan. The Double-Step experiment showed pitting which appeared to begin at the first potential of +0.1 V(SCE), which should be just above E_{pp} for Fe in this solution.

These results indicate some type of competition for active sites on the bared metal surface at potentials at which passivation should occur. The occurence of a current peak in the potentiodynamic scans at potentials just above E_{pass} for all solutions containing PC. This points to the presence of an impurity in the PC which is either electroactive itself or somehow impedes the formation and maintenance of the passive film on iron. Preliminary cyclic voltammetry and slow potential scans on Pt and Au indicate that the impurity is electroactive. The two main impurities in commercial PC (besides water) are propylene glycol and propylene oxide. Work at the present time is investigating the effect of

propylene glycol on the observed passivity in PC/water mixtures.

The capacitance of the electrochemical interface, C_{interf} , is shown as a function of solution composition in Figure 9. For Armco Fe a smooth increase is observed totaling approximately a factor of four increase in going from a totally aqueous solution to a nominally dry organic solution. Figure 10 shows the dependence of R_p on solution composition for Armco Fe. A gradual increase in the magnitude of R_p is observed with increasing PC content. This corresponds to a decrease in the general corrosion rate with increasing PC content. Due to the simultaneous increase in the capacitance with increasing PC content, the 90 and 100 mole % PC values were obtained through extrapolation of the experimentally realizable portion of the spectrum.

Analysis of the data indicates that while increasing the amount of PC in the solution lowers i_{pp} , indicating a passive film which forms more easily, the values of E_{pp} , E_{corr} and i_{pass} increase, indicating that the passive film is less protective and the environment more oxidizing. Photomicrographs of the surfaces after polarization confirm this, as in the 50 mole % PC solution, where large, hemispherical pits with electropolished bases are observed, surrounded by a surface which has undergone crystallographic attack. The 90 mole % PC had a surface which indicated classic pitting due to localized breakdown of a passive film. The large drop in i_{pass} and i_{pp} in moving from the 90 mole % PC to nominally dry PC indicates the importance of water in the dissolution of iron in PC. Inspection of the surface after polarization in the nominally dry PC did show pitting similar to that observed in the 90 mole % PC, though to a lesser extent.

Induction time studies for pitting, based upon the technique of Engell and Stolica [1], have been performed on Armco Fe in aqueous solutions containing 0.5 M $LiClO_4$. The technique involves holding the surface in the passive region (in the present case, + 0.75 V(SCE)), for a time long enough to develop a steady-state passive film thickness (in the present case, 2 hrs.), and then injecting a solution containing an aggressive species (Cl^-). The time which passes until a large increase in current is observed, indicating breakdown of the passive film, is the induction time, τ . If the induction time is measured as a function of aggressive species concentration, the reaction order of the aggressive species can be obtained. Hoar and Jacob [2] have used this technique for pitting of stainless steels in Cl^-

solutions in which they found the order of the reaction with respect to Cl^- to be between 2.5 and 4.5 depending upon the passivating potential. They took this as showing that the breakdown process involves between 2.5 and 4.5 Cl^- anions. Dalleck and Foley [3] found the order of the pitting reaction of Al 7075 to be between 2 and 8 depending upon the pH of the solution and the anion involved.

The present work on Armco Fe in 0.5 M $LiClO_4$ solution has found a reaction order of 1 for Cl^- , as shown in Figure 11. This relationship was found to hold over 4 orders of magnitude of Cl^- concentration. While more tests need to be performed in order to determine the reliability of the results, duplicate tests performed at a [Cl^-] of 10^{-3} vary by only 11 %. At the present time, this work is being extended to solutions of mixed solvent in order to develop a better understanding of the interactions between PC, water and Cl^- .

Ellipsometric experiments in 0 mole % PC and 10 mole % PC have also been performed. These experiments involved first holding the iron specimen at -0.85 V(SCE) in an effort to reduce the air-formed film, then, after obtaining steady state ellipsometric parameters, stepping the potential to +0.75 V(SCE) and recording the change in the ellipsometric parameters (Ψ and Δ) until a steady state was again reached. At that point, the electrode was again stepped to -0.85 V(SCE) in order to determine the reducibility of previously formed passive film. The measurements were taken on a manual nulling ellipsometer, and hence the time resolution was limited to approximately 2-3 minutes/point.

The results for 0 mole % PC are shown in Figures 12 and 13. Figure 12 shows the dependence of Δ on time (and, therefore, potential). The sharp discontinuities are the times at which the potential was stepped. The total change in Δ of 7 ° indicates a increase in film thickness of approximately 3.5 nm. It can also be seen that this film formed in 0.5 M $LiClO_4$ are not fully reducible, since the optical parameters do not return to their pre-passivation values. Roughening of the surface during this step may be responsible, and work to determine if that is the case is planned.

The results for the 10 mole % PC solution are shown in Figures 14 and 15 and are very similar qualitatively to the 0 mole % PC results, with the step to the passive region causing film growth and therefore a decrease in the value of Δ . The size of the decrease is much larger than in the 0 mole % PC solution (24 vs. 7 °). This indicates a much thicker film forms in the 10 mole % PC solution,

assuming that the composition of the films is the same. It should also be noted that this film seems to be totally reducible. The causes of these differences in film thickness and reducibility will be the subject of future efforts.

III. Future Work

In line with the overall objectives of the research program, the specific tasks to be pursued during Year II are listed below.

1. Determine the nature of the formation and breakdown processes of the films that form on Armco Fe, nickel, and alloys of Fe and Cr in dry PC with $LiClO_4$ as the supporting electrolyte, with the pre-existing air-formed films present.

2. Determine the nature of the formation and breakdown processes of the films that form on Armco Fe in dry PC with $LiClO_4$ as the supporting electrolyte, for bare surfaces.

3. Determine the effect of small amounts of water on the nature of the formation and breakdown processes described above.

4. Determine the influence of Cl^- ion on the formation and breakdown process in the alloy/solution combinations described above.

References

[1] H. Engell, N. Stolica, Z. Physik. Chem. N.F., v. 20, 113 (1959).

[2] T.P. Hoar, W.R. Jacob, Nature, v. 216, 1299 (1967).

[3] S. Dalleck, R.T. Foley, J. Electrochem. Soc., v. 123, 1775 (1976).

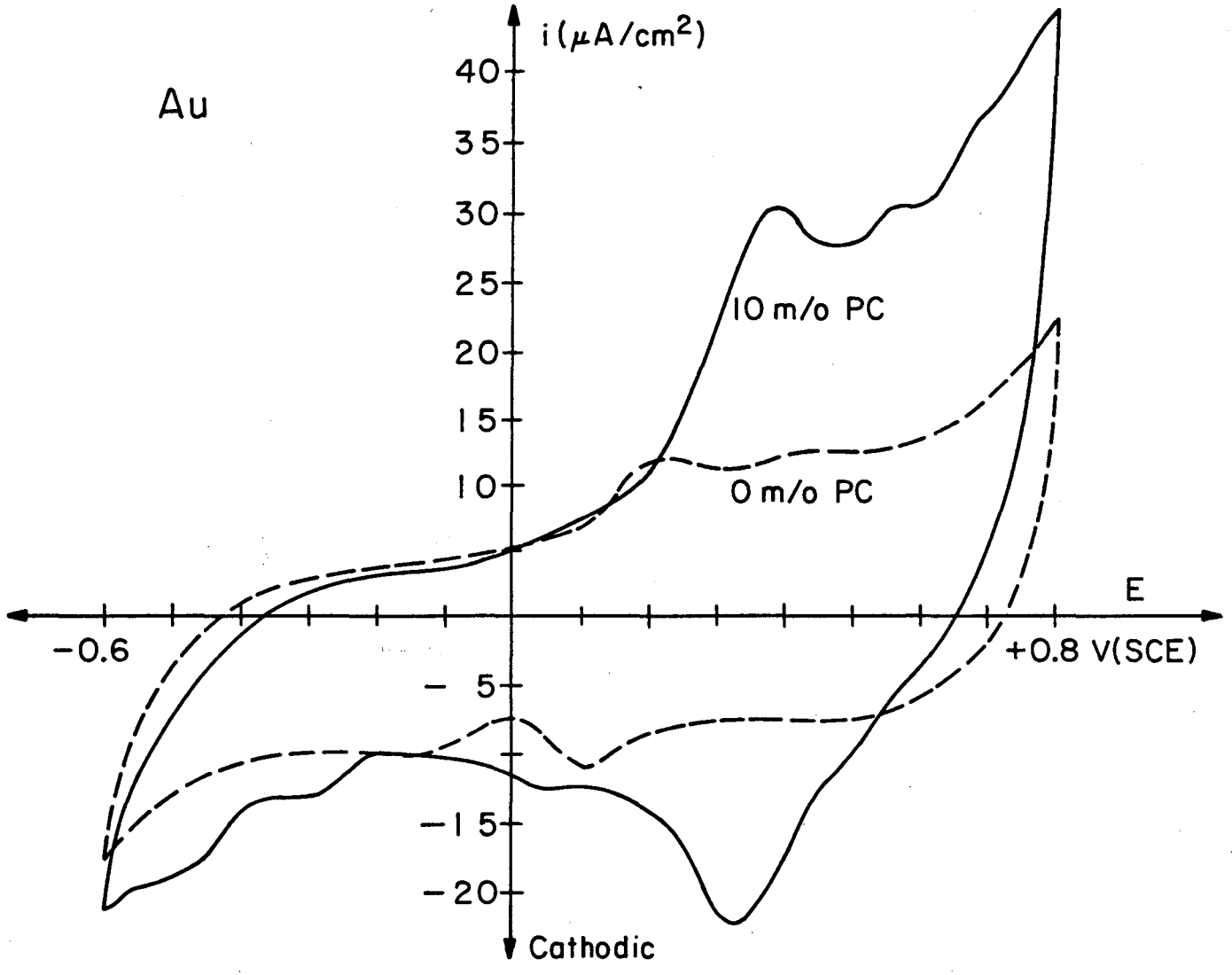

Figure 1 : Cyclic voltammogram of Au in 0.5 M $LiClO_4$ with 0 mole % or 10 mole % PC. Scan rate was 40 mV/sec.

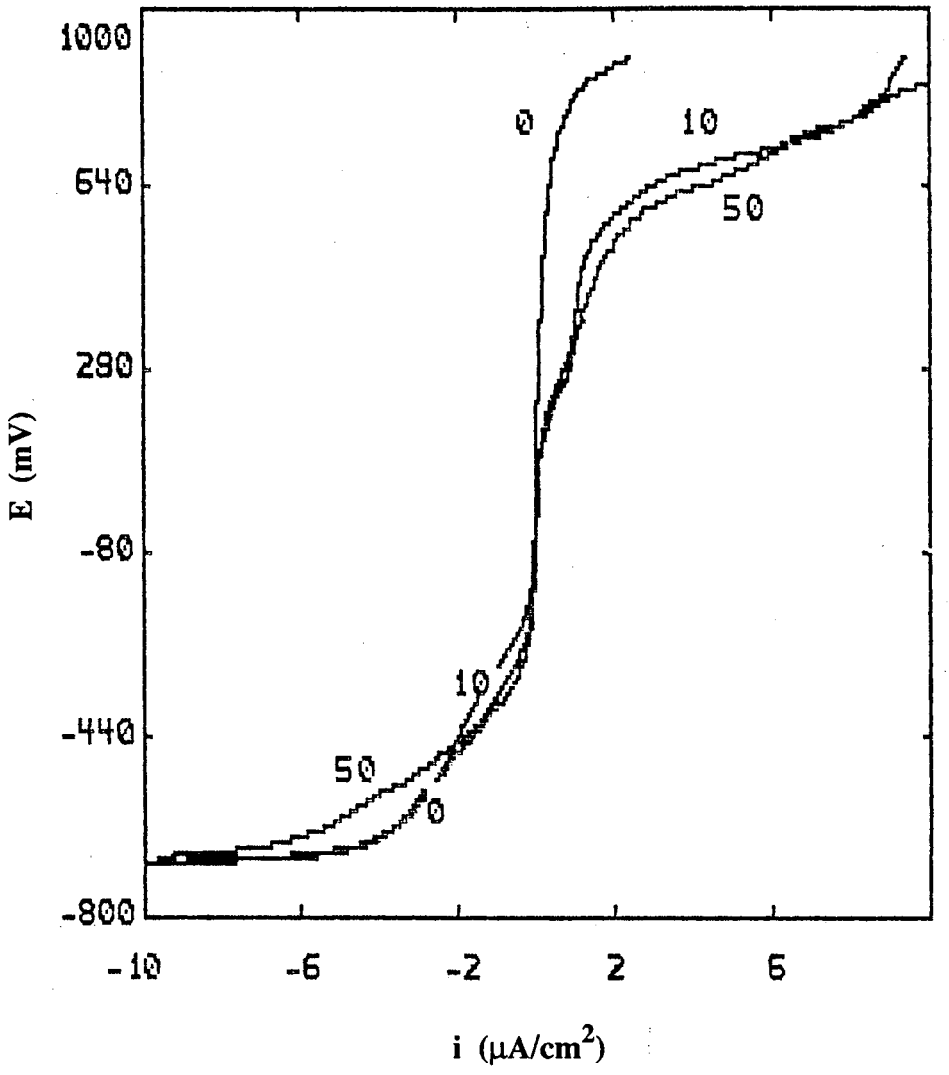

Figure 2 : Single sweep potential scans on Au in 0.5 M $LiClO_4$ with 0, 10 or 50 mole % PC. Scan rate was 0.1 mV/sec.

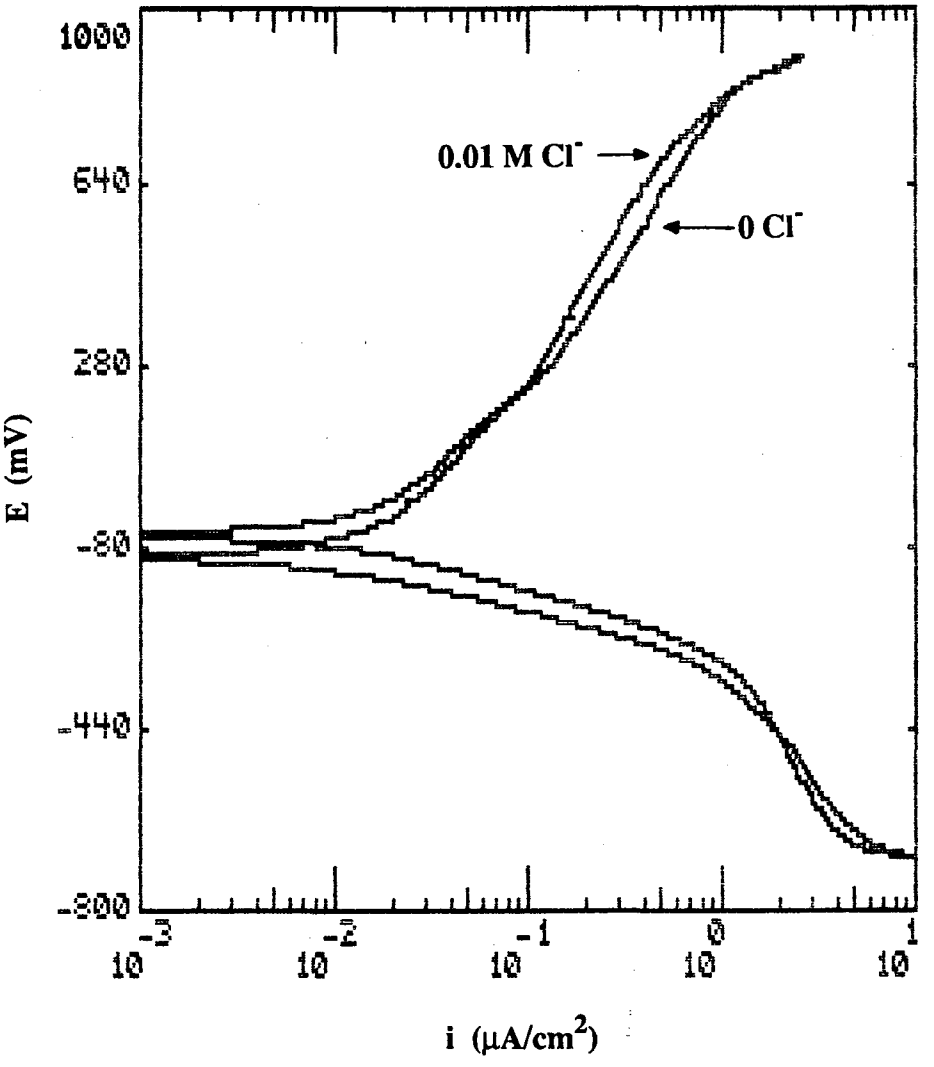

Figure 3 : Effect of Cl^- on potentiodynamic scan on Au in 0 mole % PC. Scan rate was 0.1 mV/sec.

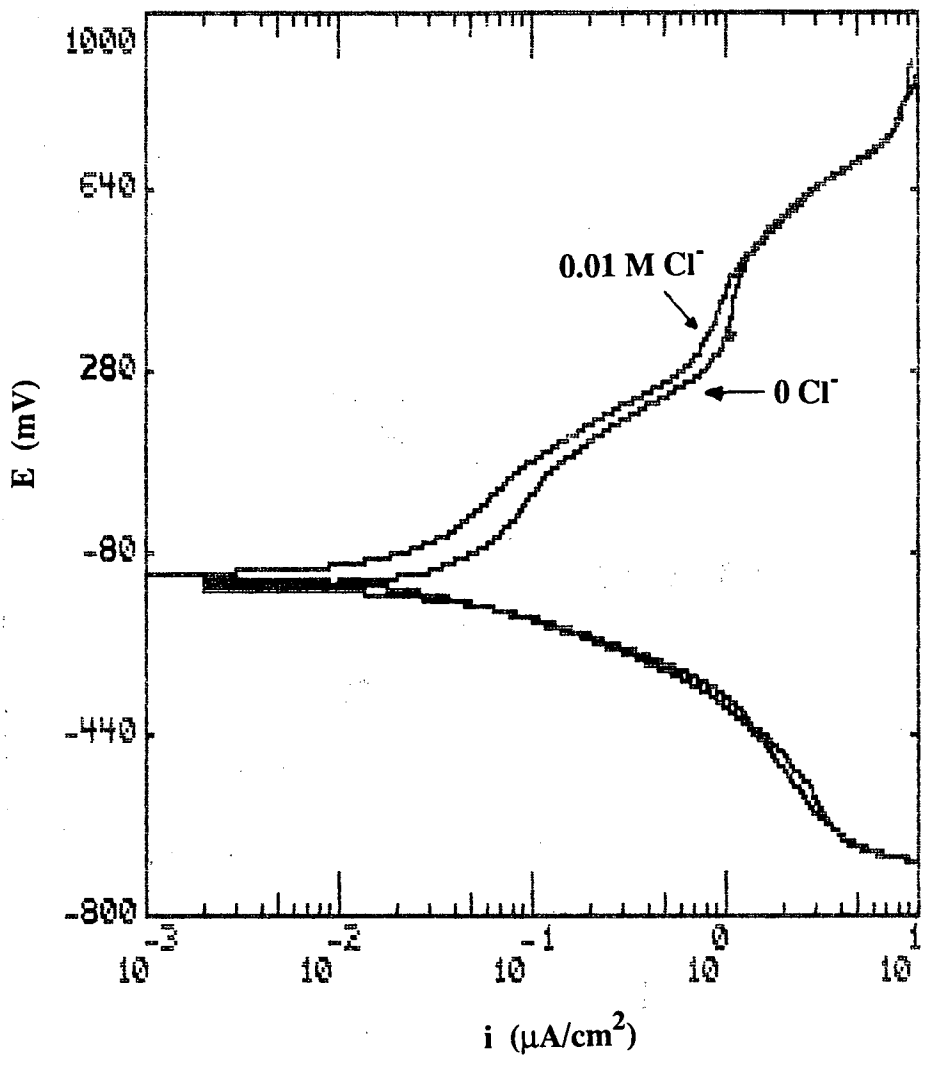

Figure 4 : Effect of Cl^- on potentiodynamic scan on Au in 10 mole % PC. Scan rate was 0.1 mV/sec.

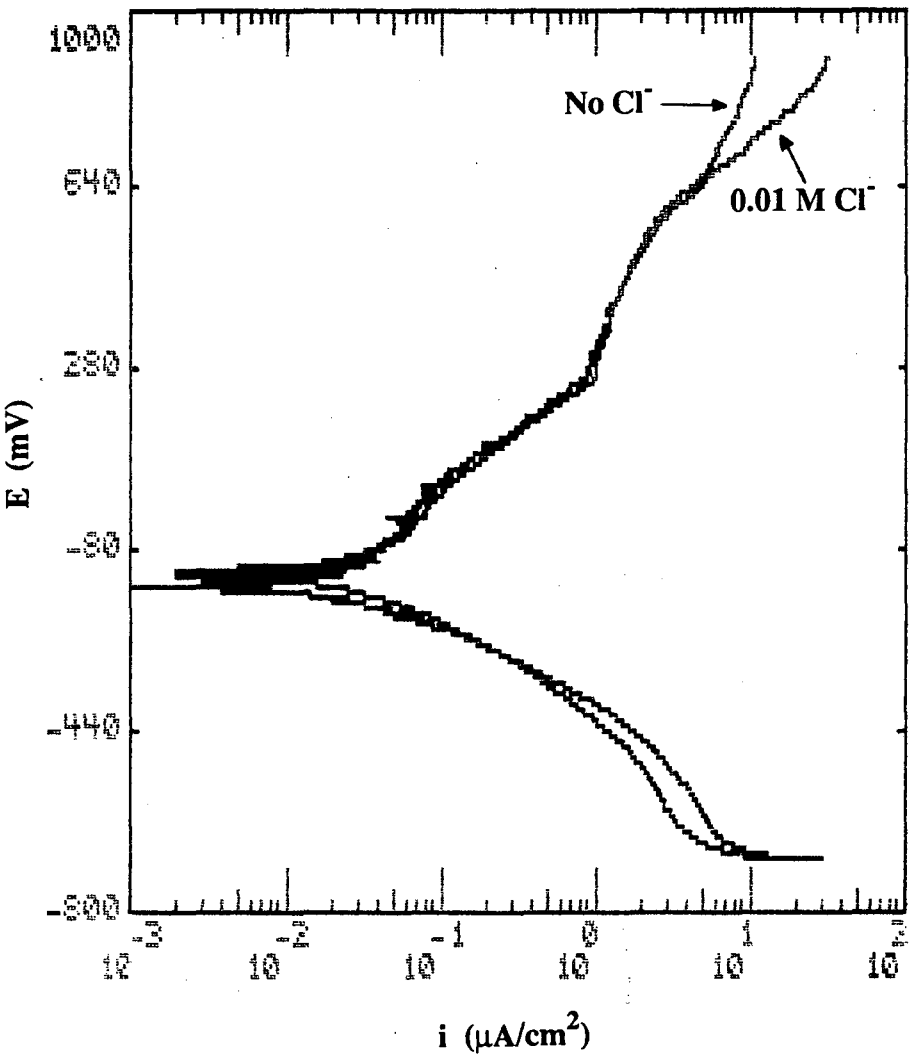

Figure 5 : Effect of Cl^- on potentiodynamic scan on Au in 50 mole % PC. Scan rate was 0.1 mV/sec.

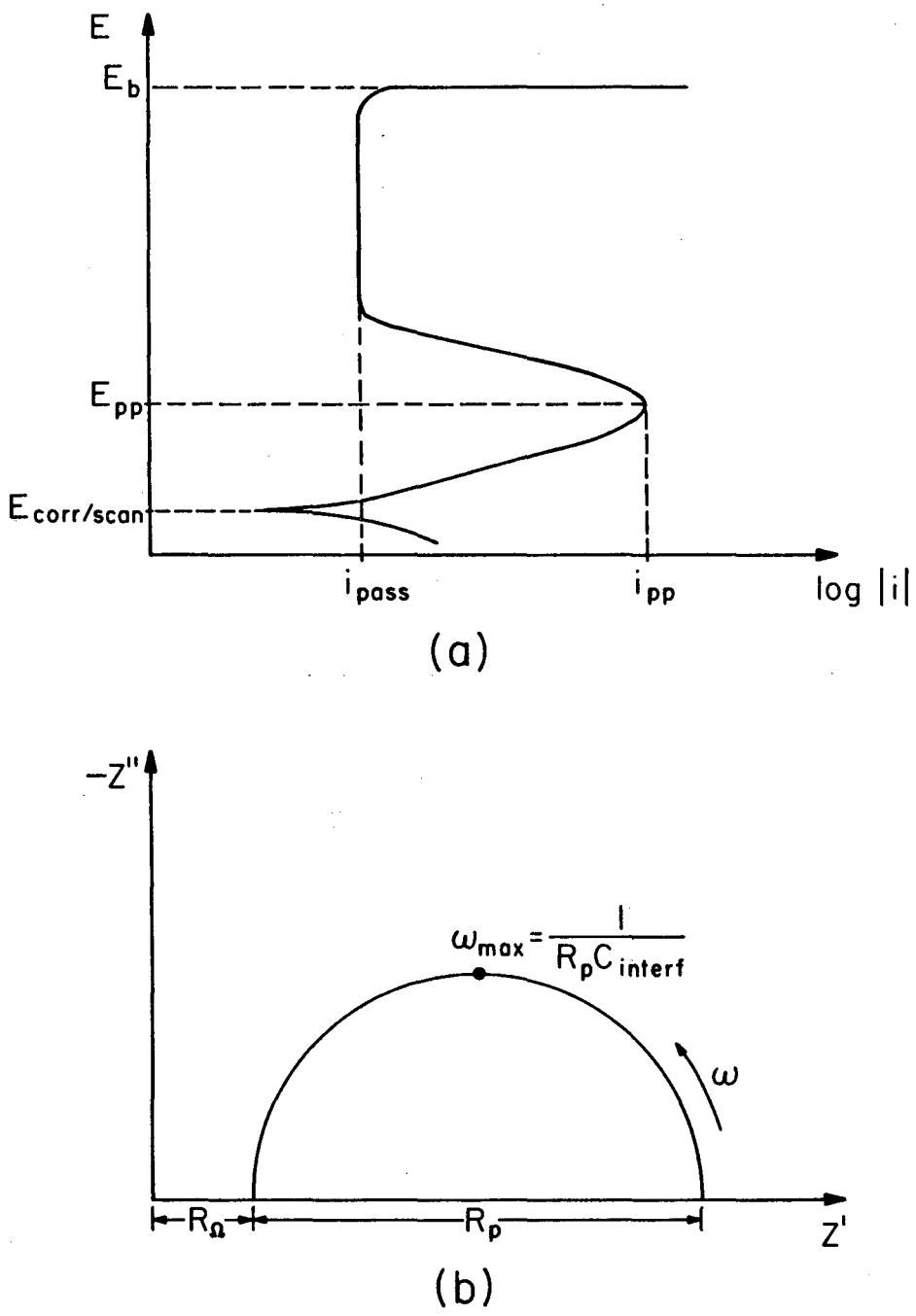

Figure 6 : (a) Schematic polarization curve indicating the characteristic potentials and currents, (b) Schematic impedance diagram, showing the characteristic impedances.

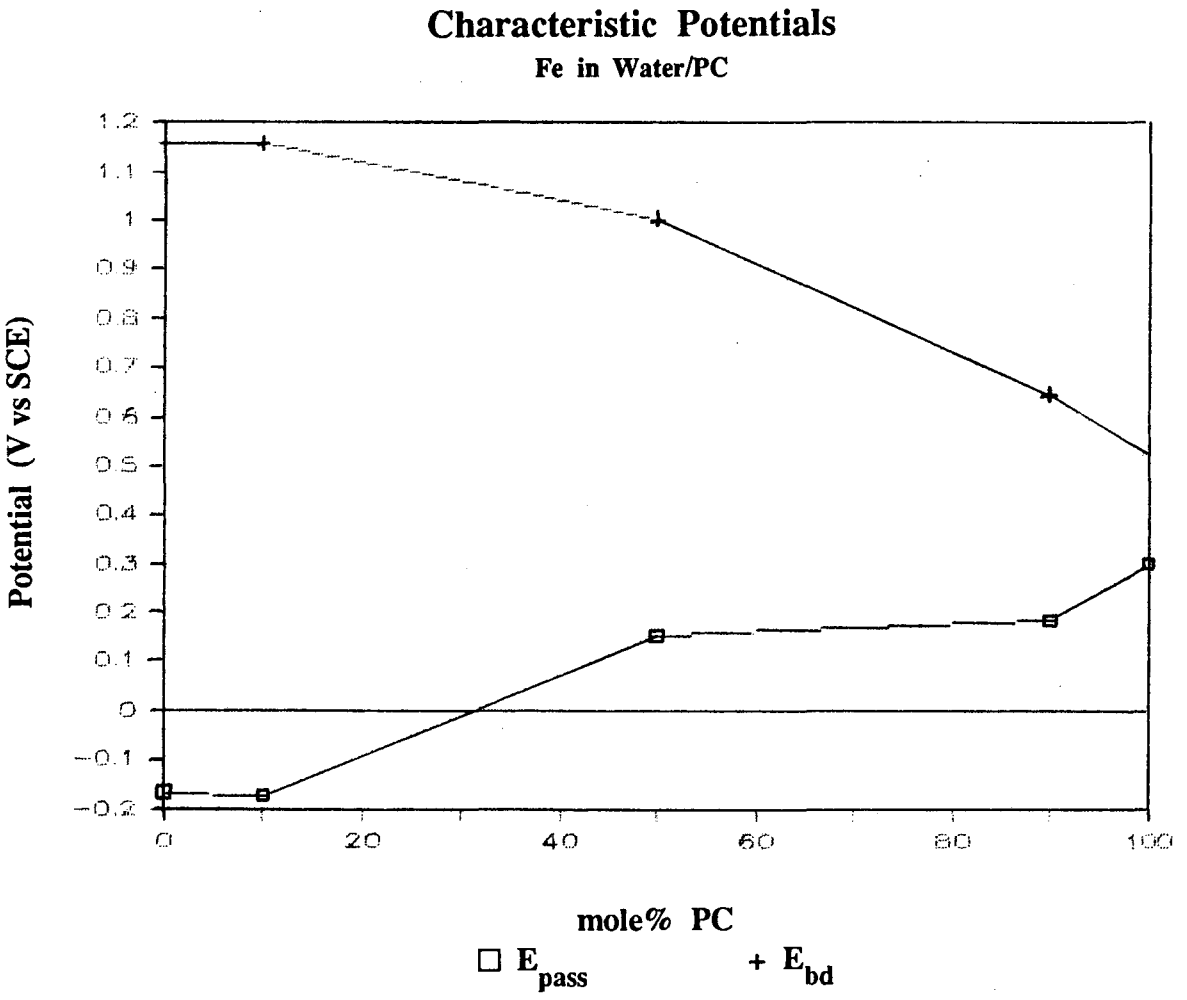

Figure 7 : Dependence of the characteristic potentials of the polarization curve on solution composition.

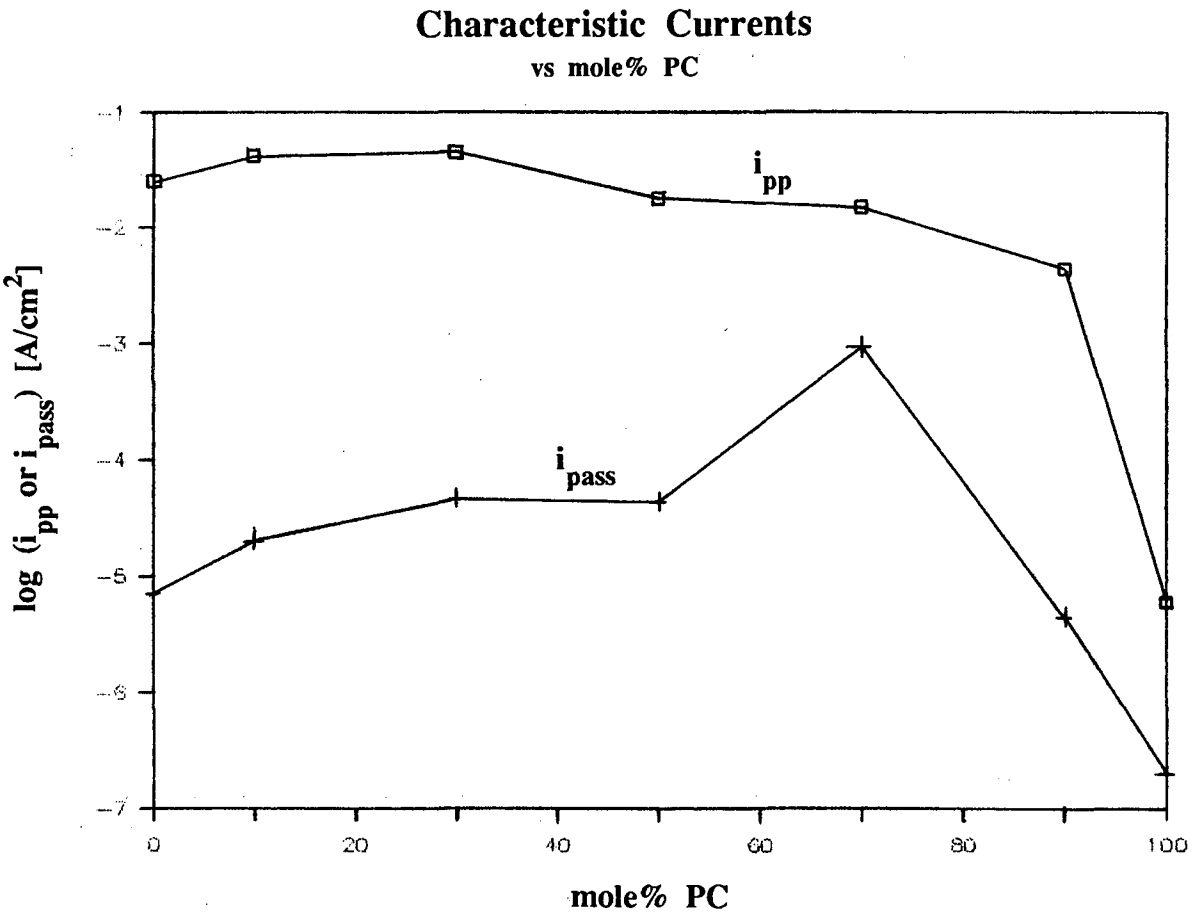

Figure 8 : Dependence of the characteristic currents of the polarization curve on solution composition.

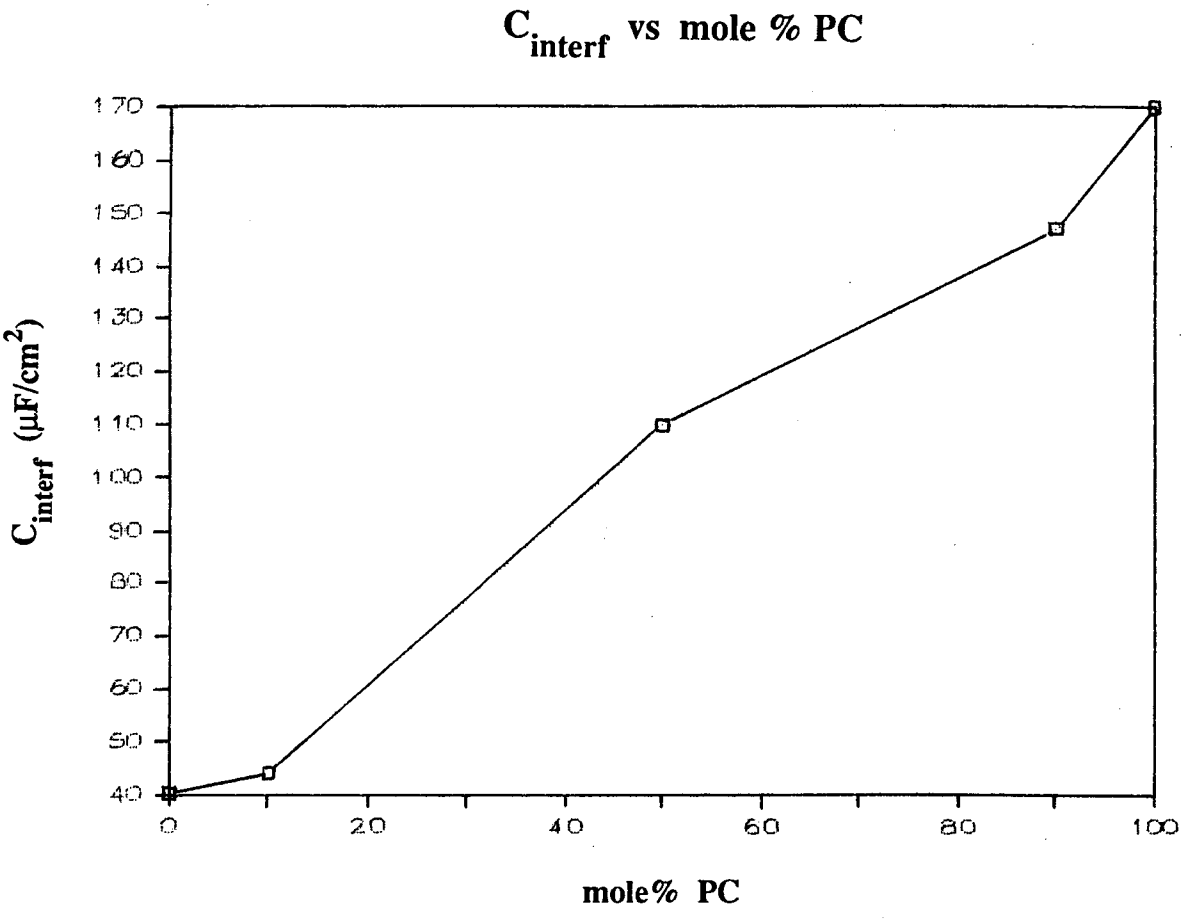

Figure 9 : Interfacial capacitance of the Armco Fe as a function of solution composition.

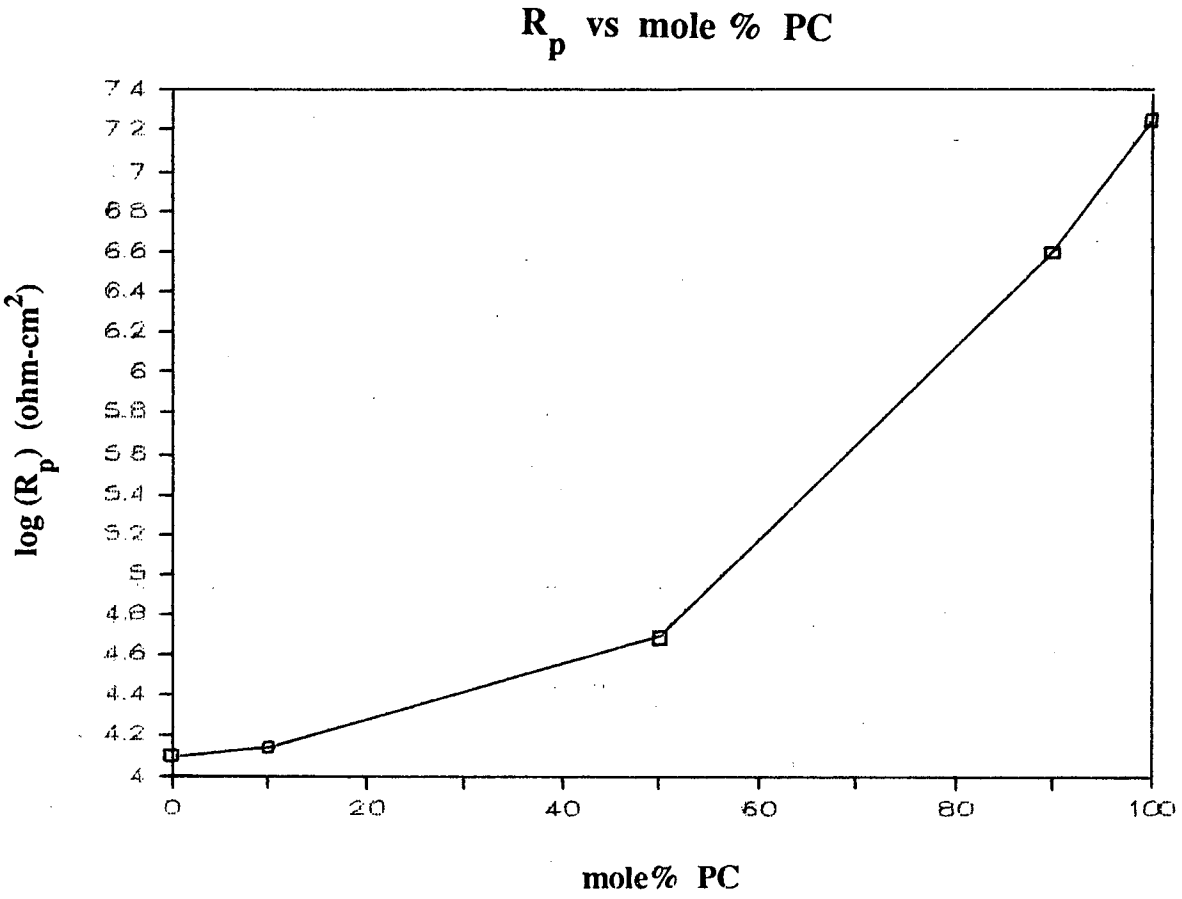

Figure 10 : Dependence of the polarization resistance of Armco Fe on solution composition.

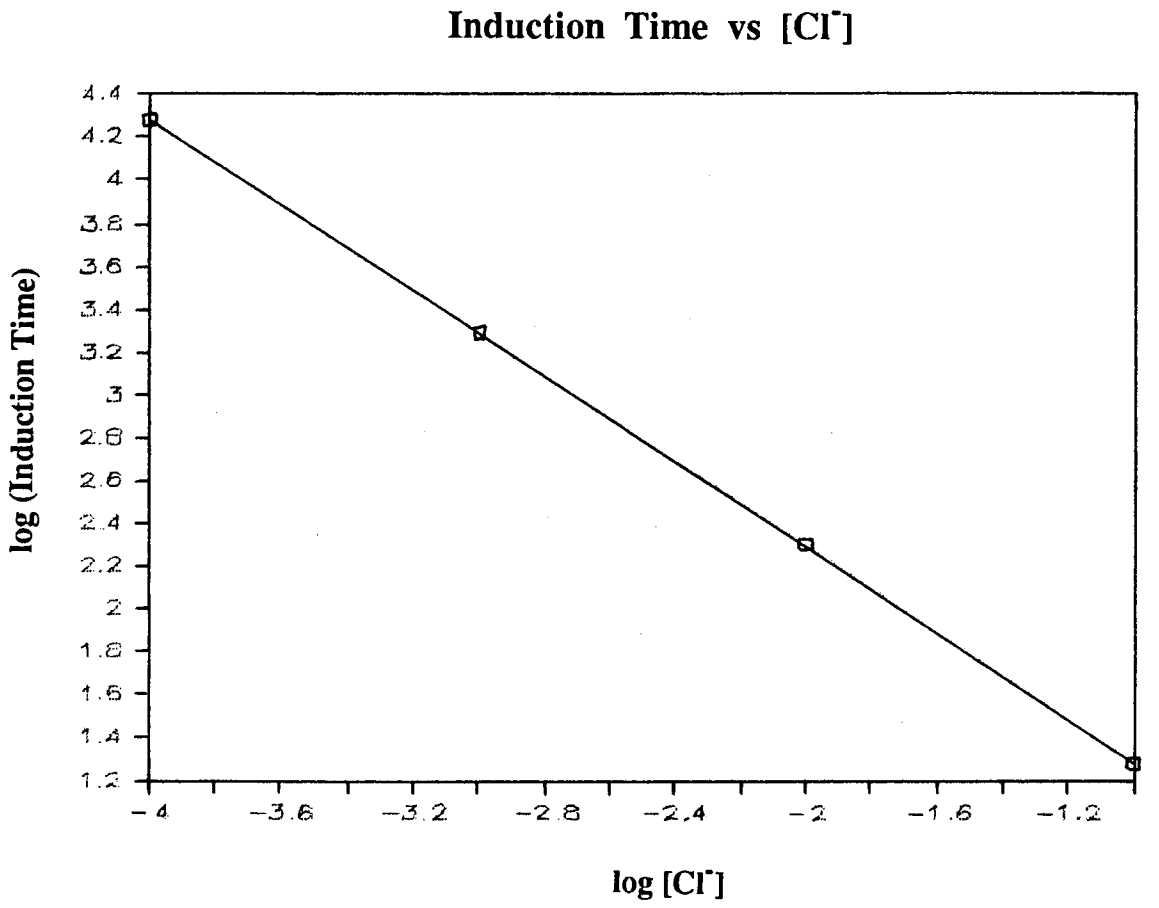

Figure 11 : Induction time for pitting for Armco Fe in aqueous 0.5 M $LiClO_4$.

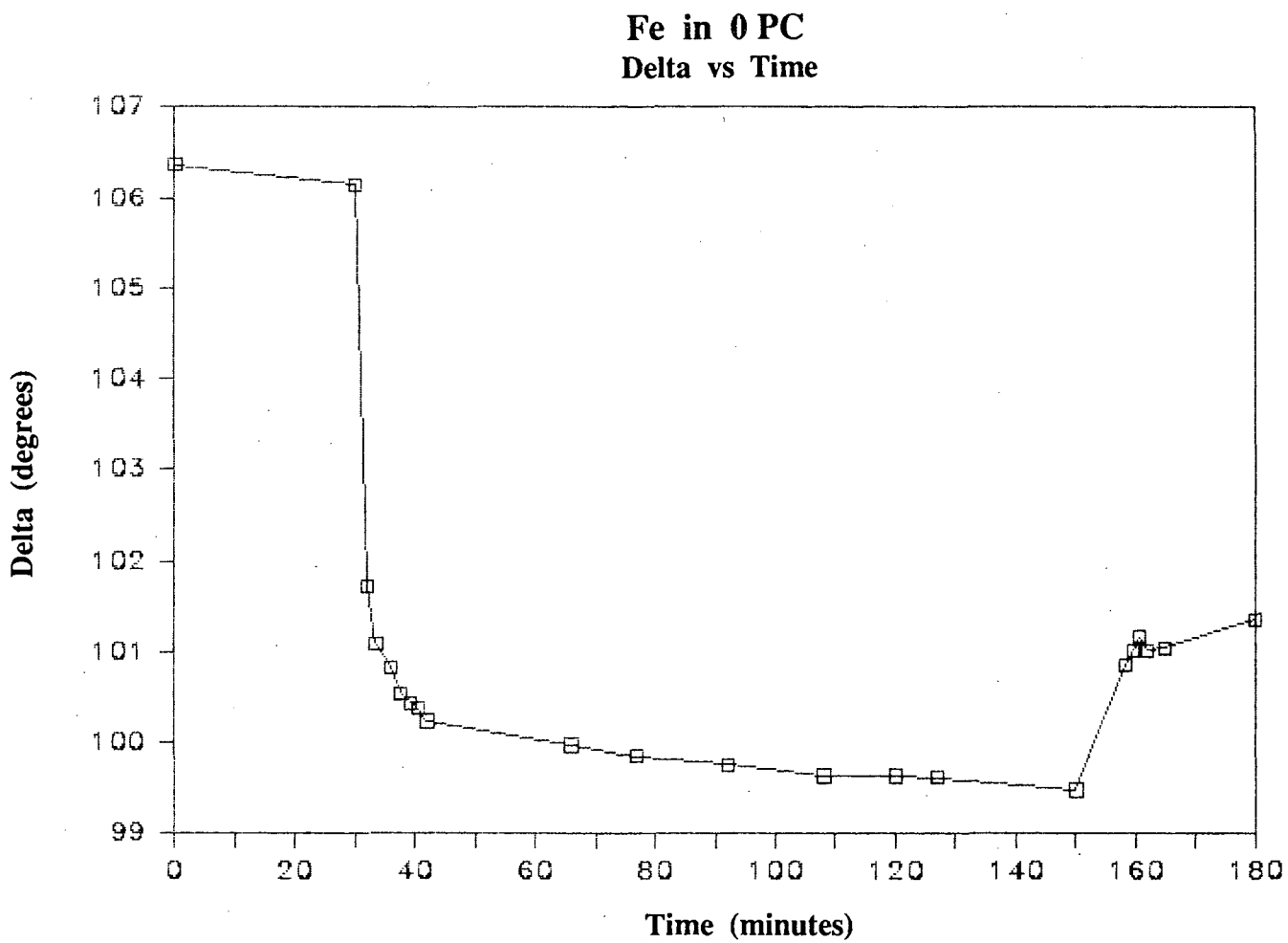

Figure 12 : Dependence of Δ on time for Fe in 0PC solution during potential stepping from -0.85 V(SCE) to +0.75 V(SCE) and back again.

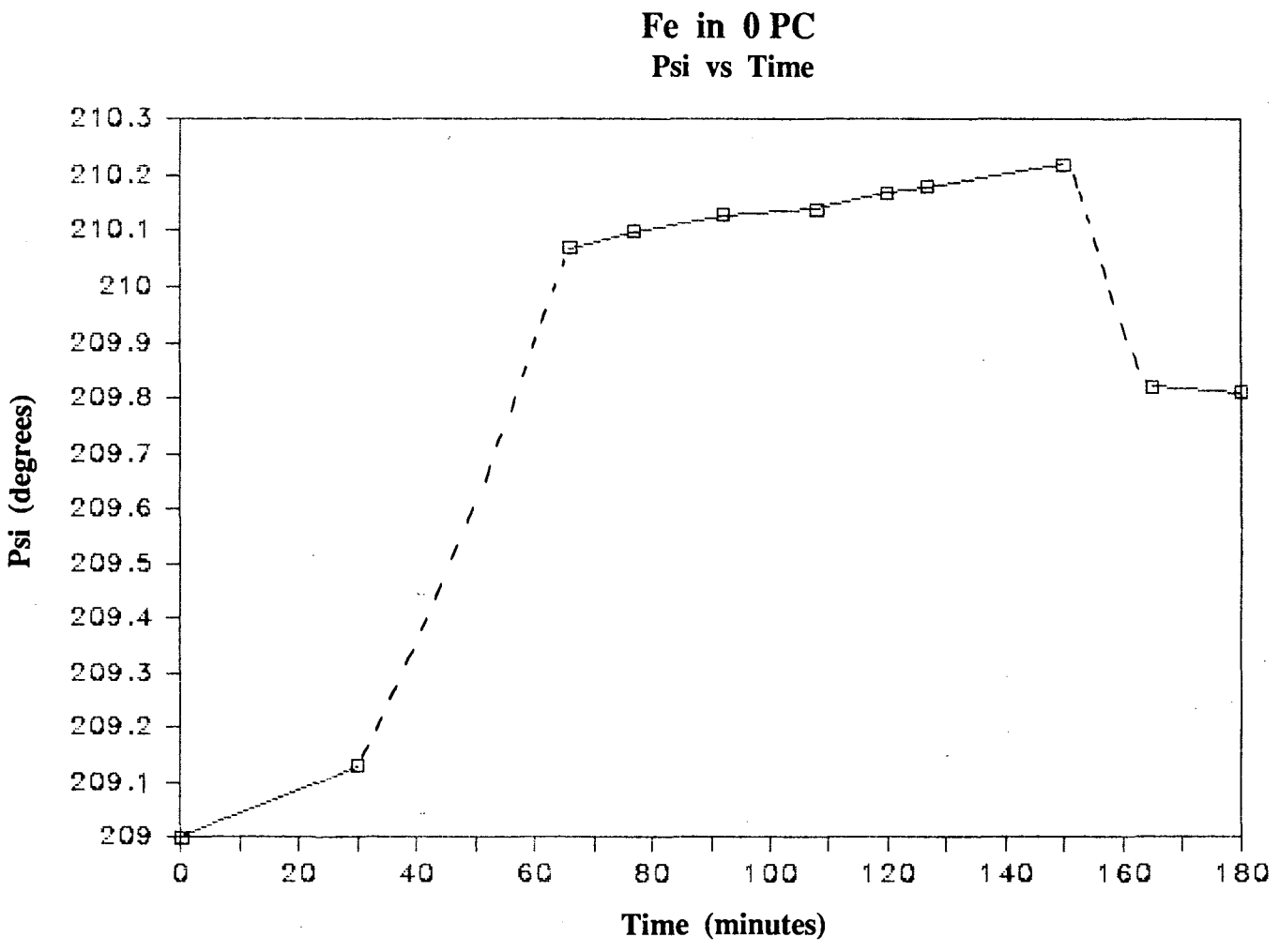

Figure 13 : Dependence of Ψ on time for Fe in 0PC solution during potential stepping from -0.85 V(SCE) to +0.75 V(SCE) and back again.

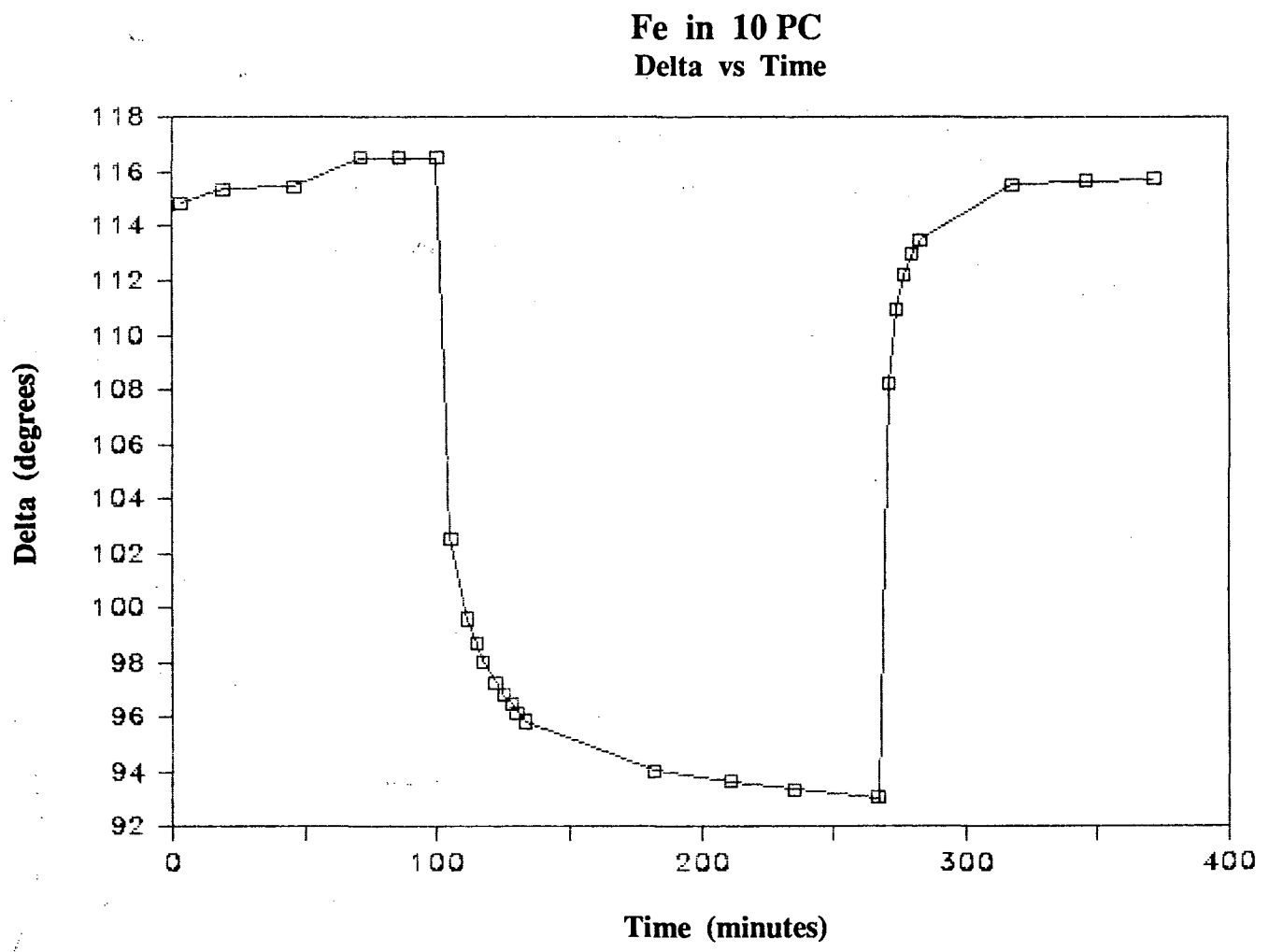

Figure 14 : Dependence of Δ on time for Fe in 10PC solution during potential stepping from -0.85 V(SCE) to +0.75 V(SCE) and back again.

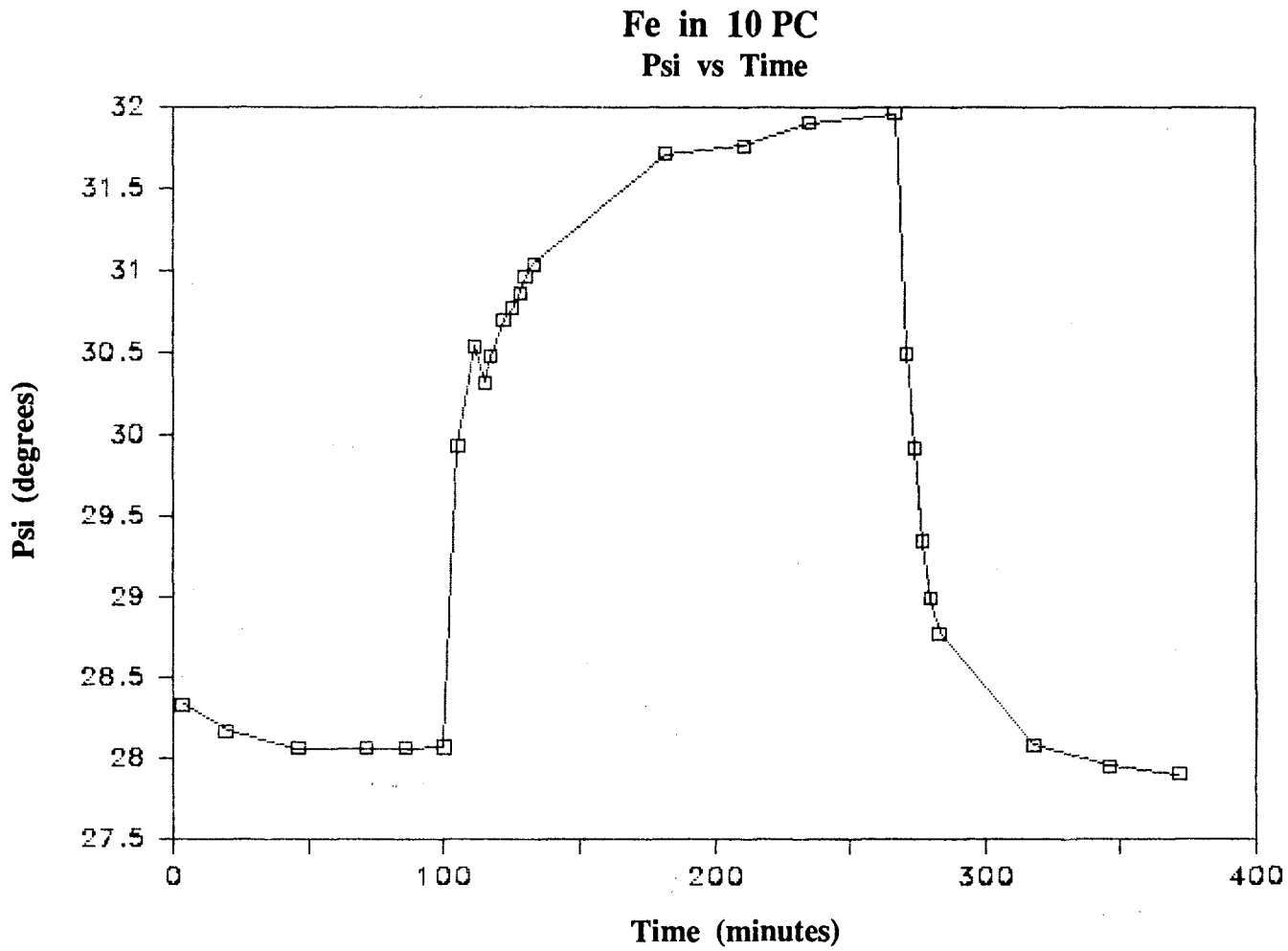

Figure 15 : Dependence of Ψ on time for Fe in 10PC solution during potential stepping from -0.85 V(SCE) to +0.75 V(SCE) and back again. breakdown process in the alloy/solution combinations described above.

LAWRENCE BERKELEY LABORATORY
TECHNICAL INFORMATION DEPARTMENT
UNIVERSITY OF CALIFORNIA
BERKELEY, CALIFORNIA 94720